frontiers | Frontiers in Molecular Neuroscience

TYPE Original Research
PUBLISHED 08 August 2025
DOI 10.3389/fnmol.2025.1636365

OPEN ACCESS

EDITED BY
Muddanna Sakkattu Rao,
Kuwait University, Kuwait

REVIEWED BY
Alice Drobny,
Evotec, Germany
Ajeena Ramanujan,
University of Texas MD Anderson Cancer Center, United States

*CORRESPONDENCE
Isabel Cardoso
✉ icardoso@ibmc.up.pt

RECEIVED 27 May 2025
ACCEPTED 25 July 2025
PUBLISHED 08 August 2025

CITATION
Saavedra J, Nascimento M, Figueira AJ, Oliveira da Silva MI, Gião T, Oliveira J, Liz MA, Gomes CM and Cardoso I (2025) Neuronal expression of S100B triggered by oligomeric Aβ peptide contributes to protection against cytoskeletal damage and synaptic loss. *Front. Mol. Neurosci.* 18:1636365. doi: 10.3389/fnmol.2025.1636365

Neuronal expression of S100B triggered by oligomeric Aβ peptide contributes to protection against cytoskeletal damage and synaptic loss

Joana Saavedra[1,2,3], Mariana Nascimento[1,2,4], António J. Figueira[5,6], Marina I. Oliveira da Silva[1,2], Tiago Gião[1,2,3], João Oliveira[1,2,7], Márcia A. Liz[1,2,8,9,10], Cláudio M. Gomes[5,6] and Isabel Cardoso[1,2,3]*

[1]i3S - Instituto de Investigação e Inovação em Saúde, Universidade do Porto, Porto, Portugal, [2]IBMC - Instituto de Biologia Molecular e Celular, Universidade do Porto, Porto, Portugal, [3]ICBAS - Instituto de Ciências Biomédicas Abel Salazar, Universidade do Porto, Porto, Portugal, [4]FMUP-Faculdade de Medicina, Universidade do Porto, Porto, Portugal, [5]BioISI-Instituto de Biosistemas e Ciências Integrativas, Faculdade de Ciências, Universidade de Lisboa, Lisbon, Portugal, [6]Departamento de Química e Bioquímica, Faculdade de Ciências, Universidade de Lisboa, Lisbon, Portugal, [7]FCUP-Faculdade de Ciências, Universidade do Porto, Porto, Portugal, [8]UMIB – Unit for Multidisciplinary Research in Biomedicine, ICBAS – School of Medicine and Biomedical Sciences, University of Porto, Porto, Portugal, [9]ITR – Laboratory for Integrative and Translational Research in Population Health, Porto, Portugal, [10]Molecular Pathology and Immunology Department, ICBAS – School of Medicine and Biomedical Sciences, University of Porto, Porto, Portugal

Alzheimer's disease (AD) is a complex neurodegenerative disorder characterized by the intracellular deposition of Tau protein and extracellular deposition of amyloid-β peptide (Aβ). AD is also characterized by neuroinflammation and synapse loss, among others. The S100 family is a group of calcium-binding proteins with intra- and extracellular functions, that are important modulators of inflammatory responses. S100B, which is upregulated in AD patients and the most abundant member of this family, was shown to inhibit *in vitro* the aggregation and toxicity of Aβ42, acting as a neuroprotective holdase-type chaperone. Although S100B is primarily produced by astrocytes, it is also expressed by various cells, including neurons. In this work, we investigated if S100B neuronal expression is triggered as a response to Aβ toxic species, to provide protection during disease progression. We used the AD mouse model AβPPswe/PS1A246E to show that neuronal S100B levels are significantly higher in 10-month-old animals, and cellular assays to demonstrate that Aβ oligomers significantly increase S100B expression in SH-SY5Y cells, but not monomeric or fibrillar Aβ. Using primary cultures of rat hippocampal neurons, we showed that S100B partially reverts Aβ-induced cofilin-actin rods (synapse disruptors), and rescues the decrease in active synapses and post-synaptic marker (PSD-95), imposed by Aβ peptide. Altogether, these findings establish the neuroprotective activity of S100B in response to proteotoxic stress in cells, highlighting its chaperone function as a crucial factor in understanding proteostasis regulation in the diseased brain and identifying potential therapeutic targets.

KEYWORDS

Alzheimer's disease, Aβ oligomers, cytoskeleton dysfunction, synapse loss, S100B, molecular chaperones, neuroprotection

1 Introduction

One of the main hallmarks of Alzheimer's Disease (AD) is the aggregation of amyloid-β peptide (Aβ) into extracellular plaques (Hardy and Higgins, 1992; Knowles et al., 2014; Selkoe and Hardy, 2016). In AD a complex self-assembly process converts monomeric Aβ into mature amyloid fibrils, comprising the formation of soluble/fibrillar oligomeric species, known as Aβ oligomers (Michaels et al., 2018) that are the responsible for disease progression (Holtzman et al., 2011; Benilova et al., 2012). Oligomers trigger the start of a series of harmful events that contribute to neuronal loss and cognitive decline (Cline et al., 2018). Examples include Tau hyperphosphorylation and missorting (Ma et al., 2009; Schützmann et al., 2021), oxidative stress (De Felice et al., 2007; Wang et al., 2014), metallostasis dysregulation (Lazzari et al., 2015; Cristóvão et al., 2016), cell membrane damage (Williams et al., 2011), axonal transport impairment (Decker et al., 2010), synaptic receptor redistribution (Lacor et al., 2007), astroglia activation (Heneka et al., 2015; Forloni and Balducci, 2018) and formation of cofilin-actin rods (Namme et al., 2021; Wurz et al., 2022; Bamburg et al., 2021). In AD, these cofilin-actin rods, structures composed of bundles of cofilin-saturated actin filaments, which result from localized cofilin hyperactivation by dephosphorylation and oxidation (Bernstein et al., 2012), inhibit intracellular trafficking and cause synaptic loss in cultured hippocampal neurons (Cichon et al., 2012; Oliveira da Silva et al., 2024).

Neuroinflammation is an important characteristic commonly present in neurodegenerative disorders, and thought to play a relevant role in AD. In its acute phase, neuroinflammation is beneficial; however, persistent activation of microglia and astrocytes, such as that caused by Aβ aggregated species, is detrimental and can contribute to AD pathogenesis. The accumulation of protein aggregates and consequent increase in inflammation results in the release of inflammatory mediators, including several alarmins (Li et al., 2011), such as Ca^{2+}-binding S100B protein (Mrak, 2001; Donato et al., 2009), which is upregulated in AD (Marshak et al., 1992) and is known to contribute to the late neuroinflammatory response (Cuello, 2017; Hagmeyer et al., 2019). In addition to its pro-inflammatory function, S100B acts as a neuroprotective holdase type chaperone by preventing the *in vitro* aggregation and toxicity of the Aβ42 (Cristóvão et al., 2018; Cristóvão et al., 2020; Rodrigues et al., 2021) and of the microtubule-associated protein Tau (Moreira et al., 2021). S100B protects cells from Aβ42-mediated toxicity, rescuing cell viability and decreasing apoptosis induced by Aβ42 in cell cultures (Cristóvão et al., 2018).

The high conservation of S100 family proteins across vertebrate species underscored their essential biological roles (Fanò et al., 1995; Gonzalez et al., 2020). S100B is the most prevalent protein in this family, constituting 0.5% of all brain proteins and 96% of the S100 proteins found in the human brain (Hernández-Ortega et al., 2024). S100B is primarily found in brain tissue, especially in astrocytes, but is also present in other cells such as enteric glia, microglia, Schwann cells, and oligodendrocytes. Furthermore, it is detected at low levels in specific neuronal populations in the cerebellum, forebrain, spinal cord, and other areas. The function of neuronal S100B and the factors that lead to its activation, and that may be linked to its neuroprotective properties, have not been fully explored. Moreover, the cellular structures that might benefit from this protection, as well as the underlying mechanisms, are not yet known. In this work, we address these aspects by testing the hypothesis that Aβ toxic species trigger neuronal S100B expression to mitigate noxious effects produced by proteotoxic Aβ over the cytoskeleton and synaptic structures.

Abbreviations: AD, Alzheimer's disease; Aβ, amyloid-b peptide; DMEM, Dulbecco's Modified Eagle Medium; FBS, Fetal bovine serum; HBSS, Hanks' balanced salt solution; HFIP, hexafluoro-2-propanol; ON, overnight; RT, room temperature.

2 Materials and methods

2.1 Proteins and peptides

Synthetic Aβ42 (GenScript) was dissolved in hexafluoro-2-propanol (HFIP; Merck) and left at room temperature (RT) for 48 h. Subsequently, the HFIP was removed using a stream of nitrogen, and the resulting powder was dissolved in dimethyl sulfoxide (DMSO; Sigma-Aldrich) at a concentration of 2000 μM. For oligomer and fibril formation, Aβ42 was diluted in F-12 medium (Alfagene) to a concentration of 100 μM and incubated for 48 h at 4°C, and for 72 h at 37°C, respectively (Costa et al., 2008). Soluble Aβ42 was obtained by diluting, at the time of use of the peptide, to the desired concentration. Human S100B was expressed in *E. coli* (BL21 (DE3) E. Cline Express, Lucigen) and purified to homogeneity as described (Ostendorp et al., 2005; Botelho et al., 2012). S100B concentrations were estimated as homodimer equivalents using UV spectroscopy at 280 nm using the theoretical extinction coefficient value of $\varepsilon_{280\,nm} = 2{,}980\ M^{-1}\ cm^{-1}$.

2.2 Transmission electron microscopy

For the examination of the structure and morphology of samples containing the different Aβ42 species, 5 μL of the samples were adsorbed into carbon-coated collodion film supported on 300-mesh copper grids (Electron Microscopy Sciences, PA, United States) and negatively stained twice with 1% (m/v) uranyl acetate (Electron Microscopy Sciences, PA, United States). Grids were visualized with a JEOL (Tokyo, Japan) JEM-1400 transmission electron microscope, operated at 80 kV, equipped with an Orious (CA, United States) Sc1000 digital camera, and exhaustively observed.

2.3 Animals

Animals were housed in a controlled environment (12-h light/dark cycles, temperature between 22 and 24°C, humidity between 45 and 65%, and 15–20 air changes/h), with freely available food and water. The AD mouse model AβPPswe/PS1A246E (Borchelt et al., 1997) was maintained on a B6/C3H/SV129 genetic background. In this study, a total of 15 animals were used, divided into three age groups: 3 months, 7 months, and 10 months ($n = 4$–6 per group). Time pregnant wild-type female Wistar rats (E18; $n = 3$) were used for the dissociated hippocampal neuronal cultures. All the experiments were approved by the Institute for Research and Innovation in Health Sciences (i3S) Animal Ethics Committee and in agreement with the animal ethics regulation from Directive 2010/63/EU.

2.4 Tissue processing

Animals were anesthetized with a mixture of ketamine (75 mg/kg) and medetomidine (1 mg/kg) administered by intraperitoneal injection, and perfused for 5 min with 40 mL of PBS. Brains were removed and fixed for 24 h at 4°C in 10% neutral buffered formalin and then transferred to a 30% sucrose solution for cryoprotection before cryostat sectioning and immunohistochemical analyses.

2.5 S100B and βIII tubulin immunohistochemistry

Free-floating 30 µm-thick coronal mouse brain sections, obtained with the cryostat, were permeabilized with 1% Triton X-100 in PBS for 15 min, at RT. After, they were washed with PBS (3x, 5 min), and incubated with 0.2 M NH_4Cl in PBS for 15 min, at RT. Next, the tissues were once again washed with PBS and blocked with 1% BSA, 1% Triton X-100 in PBS for 1 h, at RT, followed by an incubation with primary mouse anti-βIII tubulin antibody (ab7751; 1:500; Abcam) and with primary rabbit anti-S100B antibody (ab52642; 1:250; Abcam), in blocking solution, for 72 h at 4°C. After this incubation, tissues were washed with PBS (3x, 5 min) and incubated with Alexa Fluor-488 goat anti-mouse IgG antibody (A11029; 1:1500; Invitrogen) and Alexa Fluor-568 goat anti-rabbit IgG antibody (A11011; 1:1500; Invitrogen), ON at 4°C. On the next day, tissues were washed with PBS (3x, 5 min) and incubated with DAPI (1:40000; Invitrogen) for 15 min at RT. Then, tissues were washed once again with PBS (3x, 5 min). All of the previous steps were performed with agitation. The brain sections were then mounted on normafrost slides silane pre-coated (Normax), and incubated with glycerol 90% in PBS (VWR), without agitation, for 45 min at RT. For the evaluation of colocalization between S100B and βIII tubulin, the tissues were visualized and imaged using a Zeiss Axio Imager Z1 microscope equipped with an Axiocam MR3.0 camera and Axivision 4.9.1 software. Images of the cortex and hippocampus were taken using a 40x magnification objective. Two non-adjacent brain slices were used per animal, and the results are presented as the mean of these technical replicates for each mouse brain area analyzed. Negative controls were prepared in the absence of primary antibodies and showed no significant signal (data not shown).

2.6 Primary cultures of hippocampal neurons

The hippocampus was dissected from E18 rat embryos (Wistar) digested with 0.06% trypsin (Sigma-Aldrich, T4799) in Hanks' balanced salt solution (HBSS, Sigma, H9394) for 15 min at 37°C. Following digestion, neurons were dissociated by gentle trituration and resuspended in neurobasal medium (Invitrogen, 21,103,049) supplemented with 10% Fetal bovine serum (FBS), 2% N21-MAX (R&D Systems, AR008), 1% Pen-Strep and 2.5 mM L-Glutamine (Lonza, 17-605E). Cells were then counted and plated at a density of 20,000 cells/coverslip in a 24-well plate for immunostaining analysis. Coverslips (13 mm; glass; 1.5 mm thickness (Avantor)) were precoated with 20 µg/mL poly-D-lysine (Sigma, P0899). After 4 h, the medium was changed to complete medium without FBS (2% N21, 1% Pen-Strep, 2.5 mM L-Glu in Neurobasal medium).

2.7 Cofilin and βIII tubulin immunocytochemistry in primary rat neurons

DIV5 rat neurons were incubated with 10 µM Aβ42 oligomers for 48 h or at DIV6 with 5 µM S100B for 24 h; Alternatively, S100B was added halfway through the 48-h Aβ42 treatment. Neurons were fixed at DIV7 with 4% PFA in 1x cytoskeleton preservation buffer (10 mM MES pH 6.1; 138 mM KCl; 3 mM $MgCl_2$; 2 mM EGTA pH 7; 0.32 M sucrose), for 30 min at RT, and then rinsed 3x times with PBS, and incubated with −20°C methanol, for 3 min at RT. Next, cells were again rinsed 3x with PBS and incubated with blocking solution (2.5% donkey serum) in PBS containing 1% BSA (Bovine serum albumin), for 1 h at RT. This was followed by incubation with primary rabbit anti-cofilin antibody (D3F9; 1:2000; Cell Signaling) and mouse anti-βIII tubulin antibody (G712A; 1:2000; Promega), diluted in 1% BSA in PBS, overnight (ON) at 4°C. On the next day, neurons were rinsed 3x with PBS and incubated with Alexa Fluor-568 goat anti-rabbit IgG antibody (A11011; 1:1000; Invitrogen) and Alexa Fluor-488 goat anti-mouse IgG antibody (A11029;1:1000; Invitrogen), in 1% BSA in PBS, for 1 h at RT. After incubation, neurons were rinsed 3x with PBS and coverslips were mounted with FluoroshieldTM with DAPI (Sigma-Aldrich). Cell visualization and image capture was done using the Zeiss Axio Imager Z1 microscope equipped with an Axiocam MR3.0 camera and Axivision 4.9.1 software, with a 40x magnification. Finally, cells with cofilin-actin rods were manually counted and divided per total number of cells (approximately 100 cells per coverslip). Negative controls were prepared in the absence of primary antibodies and showed no significant signal (data not shown). Three independent experiments were performed in triplicate.

2.8 VGLUT1/PSD-95 immunocytochemistry in primary rat neurons

DIV12 rat neurons were incubated with 10 µM Aβ42 oligomers for 48 h or at DIV13 with 5 µM S100B for 24 h; Alternatively, S100B was added halfway through the 48-h Aβ42 treatment. Neurons were fixed at DIV 14 with 2% PFA in PBS for 3 min, on ice, and then washed with ice cold PBS, and incubated with methanol for 10 min, at −20°C. Next neurons were rinsed 3x with PBS and incubated in 0.2 M NH_4Cl in dH_2O, for 5 min, at RT, followed by another rinse 3x with PBS. Then, cells were blocked with 2% BSA, 2% FBS, 0.2% fish gelatin in PBS, for 30 min at RT. After, neurons were incubated with primary rabbit anti-VGLUT1 antibody (135B303; 1:1000; Synaptic Systems), mouse anti-PSD-95 antibody (MA1-045; 1:1000; Thermo Fisher Scientific), and guinea pig anti-βIII tubulin antibody (302,404; 1:2500; Synaptic Systems), in blocking buffer (diluted 10x), ON at 4°C. On the next day, neurons were rinsed 3x with PBS and incubated with the secondary antibodies Alexa Fluor-568 donkey anti-rabbit IgG antibody (A11011; 1:1000; Invitrogen), Alexa Fluor-647 donkey anti-mouse IgG antibody (A11029; 1:1000; Invitrogen), Alexa Fluor-488 donkey anti-guinea pig IgG antibody (706–545-148; 1:1000; Jackson ImmunoResearch), in blocking buffer (diluted 10x), for 30 min at RT. After this incubation, cells were rinsed 3 times with PBS and coverslips were mounted with FluoroshieldTM with DAPI (Sigma-Aldrich). Visualization of

cells and image capture was done using the Zeiss Axio Imager Z1 microscope equipped with an Axiocam MR3.0 camera and Axivision 4.9.1 software, with a 40x magnification. VGLUT1 and PSD-95, pre-and post-synaptic markers, respectively, were also used to the analysis of the active synapses, by assessing the colocalization of both markers. In this experiment, only one neurite per neuron was analyzed and the number of VGLUT1, PSD-95 and active synapses per neuritic length was quantified using Fiji software (Schindelin et al., 2012). An average of 30 neurons was quantified in each condition. Negative controls were prepared in the absence of primary antibodies and showed no significant signal (data not shown). Three independent experiments were performed in triplicate.

2.9 SH-SY5Y cell line

The SH-SY5Y cell line (originated from the SK-N-SH neuroblastoma cell line) was used between passages 25 and 30, and cultured in Dulbecco's Modified Eagle Medium (DMEM) F12 (Alfagene) supplemented with 10% FBS (Gibco) and 1% Pen-Strep and cells were incubated at 37°C in a humidified atmosphere with 5% of CO_2. The medium was changed every 2–3 days.

2.10 Treatment of SH-SY5Y with Aβ42

SH-SY5Y cells were studied under different conditions including incubation with 10 μM Aβ42 soluble, oligomeric or fibrillar, different concentrations of oligomeric Aβ42 (1–10 μM), and for different time periods (12, 24 and 48 h). After incubation, cells were analyzed by real-time qPCR, immunocytochemistry, while supernatants were investigated by slot blot.

2.11 Real-time qPCR

SH-SY5Y cells were homogenized with trizol reagent (Ambion) for 5 min at RT, and transferred to an eppendorf. Then, chloroform (Sigma) was added (0.2 mL of chloroform for each 1 mL of trizol), and the eppendorfs were shaken for 15 s, followed by a 2–3 min incubation at RT. After centrifugation at 12000 g, for 15 min, at 4°C, the upper phase was collected in a new eppendorf. Isopropanol (Sigma; 0.5 mL of isopropanol for each 1 mL of trizol) was added, followed by a 10 min incubation at RT. After another centrifugation at 14000 g for 20 min at 4°C, the supernatant was discarded, and the pellet was resuspended in 75% ethanol (1 mL of ethanol for each 1 mL of trizol), followed by centrifugation at 7500 g for 5 min at 4°C. The supernatant was once again discarded and the ethanol was allowed to completely evaporate. The pellet was resuspended in 15–20 μL of DEPC-Water (Fisher Scientific) and left for 10 min at 60°C.

RNA concentration and purity were determined using a NanoDrop photometer (Thermo Fisher Scientific) by measuring the absorbance at 260 nm for RNA concentration, and the A260/A280 ratio for RNA purity assessment.

Subsequently, 2 μg of RNA were reverse-transcribed into cDNA using NZY First-Strand cDNA Synthesis kit (NZYtech) and the resulting cDNA was saved at −20°C until used. The analysis of the expression of the S100B gene was conducted using Real-Time Polymerase Chain Reaction (RT-qPCR). The actin gene was used as an internal control for normalization. The RT-qPCR reaction mixture was prepared with the SYBR green reporter (iQ SYBR green supermix, BioRad), following the manufacturer's instructions.

The PCR primers used were hActin (Forward: 5'ACAGAGCCTCG CCTTTGCCG; Reverse: 5'CACCATCACGCCCTGGTGCC) and hS100B (Forward: 5'AGAGCAGGAGGTTCTGGA; Reverse: 5'TCGT GGCAGGCAGTAGTA) and conditions used were initial denaturation 95°C 3 min, denaturation and annealing (40 cycles) 95°C during 10 s and 60°C during 30 s, melt curve 65°C to 95°C (increment 0.5°C for 5 s). The RT-qPCR was carried out using the CFX96 Touch Real-Time PCR Detection System (BioRad). The relative quantification was performed using the comparative method (2-ΔΔct; Livak and Schmittgen, 2001). Two independent experiments were performed in triplicate.

2.12 Slot blot

To perform the slot blot analysis, 1 mL of SH-SY5Y culture supernatant was used and applied to the slot blot manifold. The samples were drawn by vacuum through a pre-wetted nitrocellulose membrane (0.2 μm thickness; GE Healthcare Life Science). Then, the membrane was blocked for 1 h with 5% milk in PBS, at RT, and then incubated with the primary rabbit anti-S100B antibody (1:1000; Abcam) in 3% milk, ON at 4°C. On the next day, the membrane was washed with PBS-T (3x, 5 min) and incubated with the secondary rabbit antibody HRP (1:2500; Binding Site), for 1 h at RT. After washing again, the membrane with PBS-T (3x, 5 min), the blot was developed using ClarityTMWestern ECL substrate (Bio-Rad), and S100B was detected and visualized using a chemiluminescence detection system (ChemiDoc, Bio-Rad).

2.13 S100B immunocytochemistry and staining with Phalloidin iFluor-488

After fixation, SH-SY5Y cells were washed with PBS (3x, 5 min) and permeabilized with 0.1% Triton X-100 in PBS for 10 min at RT. Cells were once again washed with PBS (3x, 5 min) and blocked with 5% BSA in PBS for 1 h, then incubated with primary rabbit anti-S100B antibody (ab52642; 1:200; Abcam) in 1% BSA in PBS, ON at 4°C. On the next day, cells were washed with PBS (3x, 5 min) and incubated with Alexa Fluor-568 goat anti-rabbit IgG antibody (A11011; 1:1500; Invitrogen) with 1% BSA in PBS for 1 h at RT, and then washed once again with PBS (3x, 5 min) and incubated with Phalloidin iFluor-488 (1:100; Abcam) in 1% BSA in PBS, for 1 h at RT. After this incubation cells were rinsed with PBS and coverslips were mounted with FluoroshieldTM with DAPI (Sigma-Aldrich). Cell visualization and image capture were done using the Zeiss Axio Imager Z1 microscope equipped with an Axiocam MR3.0 camera and Axivision 4.9.1 software, with a 40x magnification. Fluorescence mean intensity per area in the images was quantified using Fiji software (Schindelin et al., 2012). Negative controls were prepared in the absence of primary antibodies and showed no significant signal (data not shown). At least two independent experiments were performed in triplicate.

2.14 Statistics

All quantitative data were expressed as mean ± standard error of the mean (SEM). Initially, data was assessed whether it followed a Gaussian distribution. The Shapiro–Wilk test was used to assess the normality of the data and established that all data followed a normal distribution. Differences among conditions or groups were analyzed by one-way ANOVA with the appropriate *post hoc* pairwise tests for multiple comparisons tests. *p*-values lower than 0.05 were considered statistically significant. Statistical analyses were carried out using GraphPad Prism 8 software for Windows.

3 Results

3.1 Neuronal expression of S100B in the cortex increases with age

To evaluate the variation of S100B levels along the AD continuum, we resorted to the AD mouse model AβPPswe/PS1A246E bearing two AD-related transgenes (APP and PSEN1) and in which Aβ deposition starts at about the age of 6 months (Oliveira et al., 2011). To investigate this, we analyzed S100B expression in animals aged 3, 7, and 10 months, representing pre-symptomatic, early amyloid deposition, and advanced disease stages, respectively. The results showed a progressive increase in S100B expression in the cortex with age, reaching significantly higher levels at 10 months compared to 3 months (Figure 1A). In contrast, no differences were observed in the hippocampus (Figure 1A). These findings align with the documented elevation of S100B levels in advanced stages of AD.

Although S100B is a widely recognized astrocytic protein, some studies also report its expression in neurons (Hagmeyer et al., 2019), albeit at lower levels. Given that S100B suppresses both Aβ and Tau aggregation (Cristóvão et al., 2018; Moreira et al., 2021), we hypothesized that its neuronal expression could partially contribute to the observed protective effect. To investigate this, we analyzed neuronal expression of S100B in the cortex, where differences were observed for total S100B, by assessing its colocalization with βIII-tubulin, a neuronal marker. The results revealed a significant increase in neuronal S100B expression in 10-month-old animals compared to both 3- and 7-month-old animals (Figure 1B). Although it seems unlikely that the increase in total S100B is only due to neuronal expression, our results indicate that neuronal S100B expression indeed rises with disease progression.

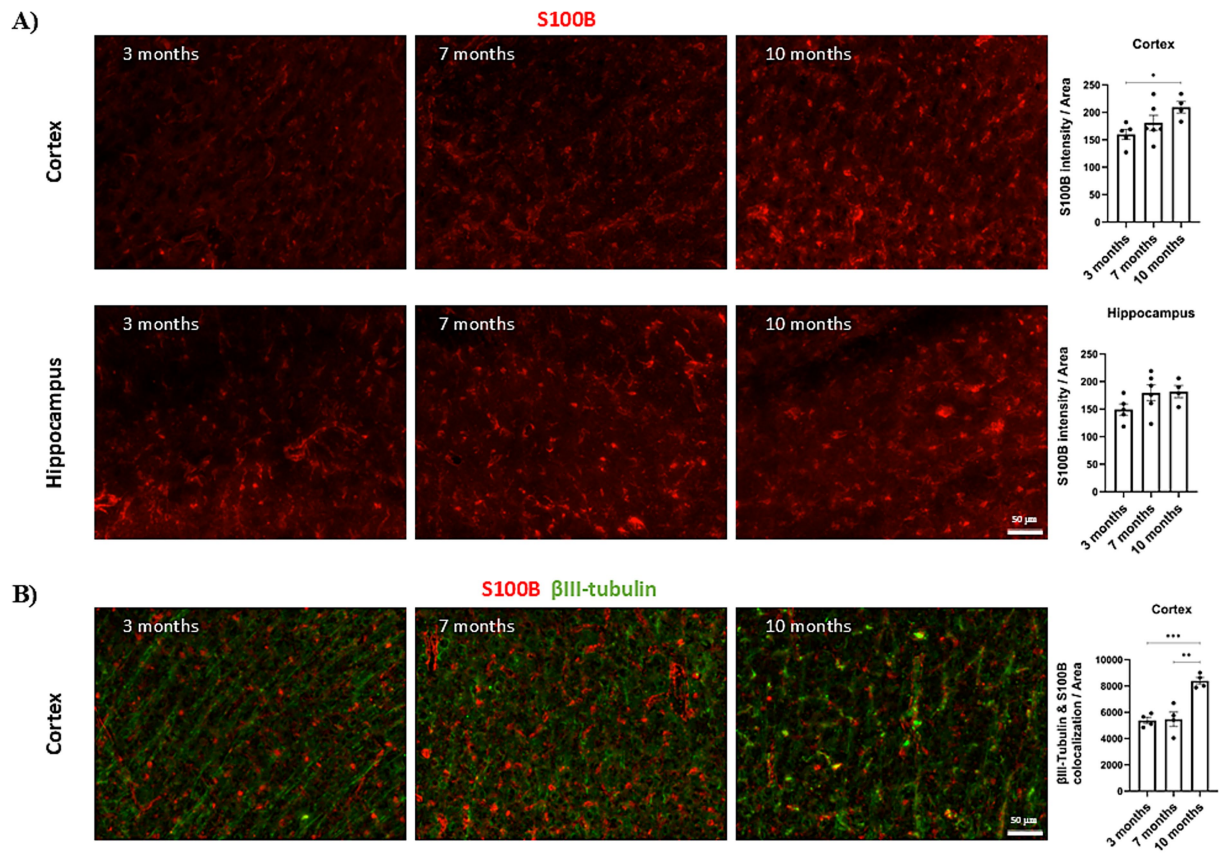

FIGURE 1
Expression of S100B in the AβPPswe/PS1A246E AD mouse model at 3, 7 and 10 months. **(A)** Representative images and quantification plots of S100B expression in AD mice at 3 (n = 5), 7 (n = 6) and 10 (n = 4) months, showing significant differences between 10-month-old animals when compared with 3-month-old animals in the cortex. **(B)** Representative images and quantification plot of S100B colocalization with βIII-tubulin showing a significantly increase in 10-month-old animals (n = 4) when compared with 3- (n = 4) and 7- (n = 4) month-old animals. Red: S100B; Green: βIII-tubulin. Scale bar = 50 μm. Data are expressed as mean ± SEM.*p < 0.05; **p < 0.01; ***p < 0.001.

3.2 Aβ oligomers induce an increase in S100B levels in the SH-SY5Y cell line

To investigate whether S100B neuronal expression is a protective response to the elevated Aβ levels observed in these animals, we conducted experiments using the SH-SY5Y cell line. Cells were treated with different Aβ species (10 μM, soluble, oligomers and fibrils; Figure 2A), and only Aβ oligomers were found to trigger S100B expression, both at protein (Figure 2B) and transcript levels (Figure 2C). Although the preparations of Aβ species are naturally heterogenous, each one is enriched in the respective species. Subsequently, we tested varying concentrations of Aβ oligomers (1, 2.5, 5 and 10 μM) for 24 h, with 10 μM Aβ oligomers significantly increasing S100B expression compared to control cells (Figure 2D). To further refine these observations, we examined the effect of incubation duration with 10 μM Aβ oligomers (0, 12, 24 and 48 h) finding that S100B expression peaked at 24 h (Figure 2E). Additionally, we evaluated whether Aβ oligomers influence S100B secretion by analyzing the supernatants of cells incubated with 10 μM Aβ oligomers for 24 h. The results revealed increased levels of secreted S100B (Figure 2F), corroborating the role of Aβ oligomers in upregulating S100B expression. Altogether, these findings suggest that neuronal S100B expression may serve as a response to Aβ oligomers.

3.3 S100B reverts cofilin-actin rod formation induced by Aβ42 oligomers in rat primary hippocampal neurons, protecting against cytoskeleton damage

Cofilin-actin rods are cytoskeleton inclusions that form in response to toxic stimuli, such as chemical or physical stress. These protein inclusions are often associated with neurodegenerative diseases, and their formation has been observed not only *in vitro* (Maloney et al., 2005), but also in human AD brains (Sisodia and Price, 1995) as well as in the AD mouse model used in this work (Supplementary Figure 1). Their formation disrupts normal neuronal cytoskeleton function, leading to compromised neuronal processes and overall cellular dysfunction.

To further explore whether S100B, which is either expressed or internalized by neurons (Supplementary Figure 2), can mitigate toxic effects of Aβ, primary rat hippocampal neuron cultures were used to assess cofilin-actin rods formation. Neurons were exposed to Aβ oligomers (10 μM) for 48 h to induce rod formation, with S100B (5 μM) added at the 24-h mark to evaluate its protective effects. Cells with rods were counted and the results demonstrated that S100B partially rescued the Aβ-induced phenotype, while S100B alone had no impact on rod formation (Figure 3, quantification plot). It is worth noting that previous studies have shown that S100B concentrations of up to 30 μM do not impair neuronal viability (Hagmeyer et al., 2018).

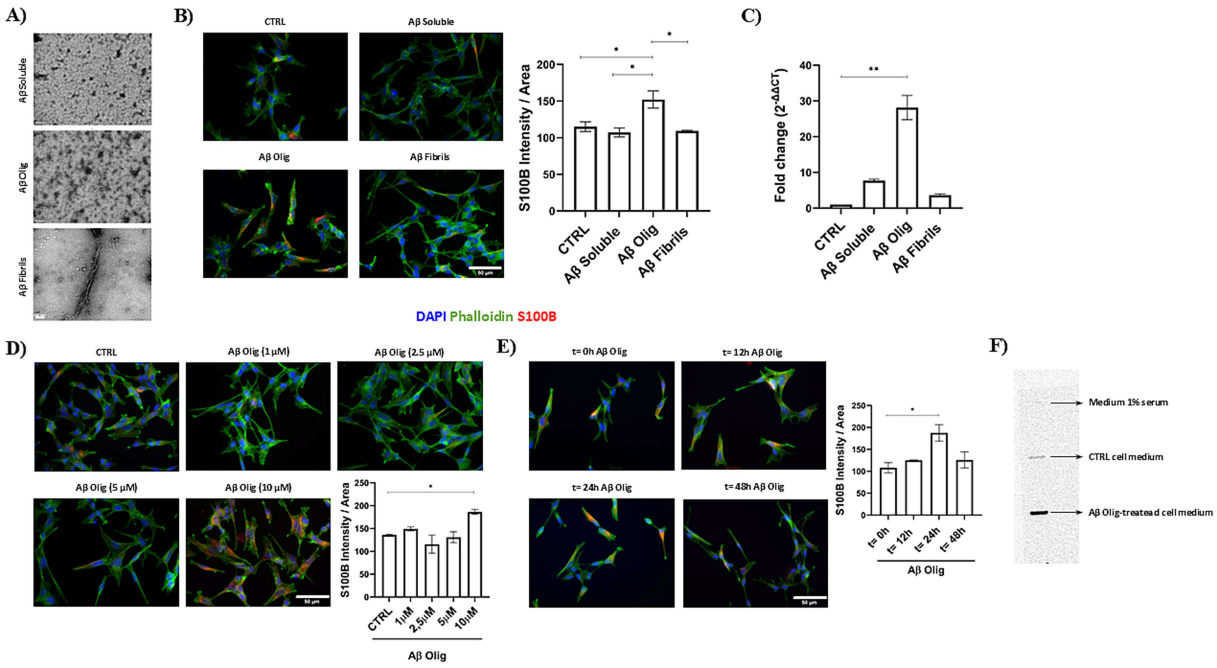

FIGURE 2
Impact of Aβ oligomers in S100B expression in SH-SY5Y cells. **(A)** TEM images of the different Aβ species (soluble, oligomeric (AβOlig) and fibrillar) used in SH-SY5Y treatments. Representative images and quantification plots of cells treated with 10 μM Aβ species (soluble, oligomeric and fibrillar), displaying different effects regarding S100B expression, with only oligomers increased S100B, both **(B)** protein and **(C)** transcript. Representative images and quantification plots of **(D)** cells treated with different concentrations (1, 2.5, 5, 10 μM) of Aβ oligomers for 24 h, showing a significant increase of S100B in cells treated with Aβ oligomers at 10 μM, and **(E)** cells incubated with Aβ oligomers 10 μM for different periods of time, evidencing increased S100B in cells incubated for 24 h, as compared to 0, 12 and 48 h. **(F)** 24 h- conditioned media, analyzed by slot blot, from cells control (Control cell medium), treated with 10 μM Aβ oligomers (Aβ Olig-treated cell medium), showing that Aβ oligomers induced increased secretion of S100B into the media. Fresh medium was used as negative control (medium 1% serum). Blue: DAPI; Green: Phalloidin; Red: S100B. Cells Scale bar = 50 μm. TEM Scale bar = 100 nm. Data are expressed as mean ± SEM. *$p < 0.05$; **$p < 0.01$.

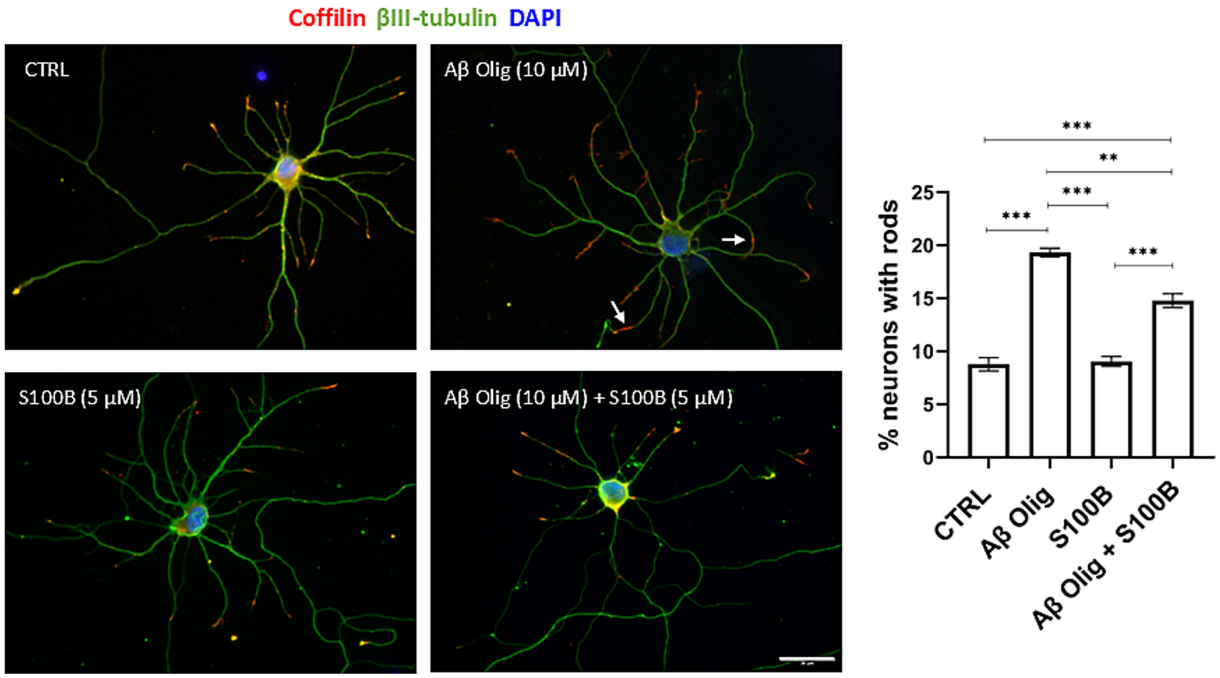

FIGURE 3
Effect of Aβ oligomers and impact of S100B in cofilin-actin rod formation in primary cultures of rat hippocampal neurons. Representative images and quantification plots of rat hippocampal neurons (DIV7) showing increased % of cells with cofilin-actin rods after incubation with Aβ oligomers (Aβ Olig, 10 μM). S100B (5 μM) added after 24 h partially rescued the Aβ-induced phenotype. S100B alone did not produce alterations, as compared to control (CTRL). White arrow points out one cofilin-actin rod. Green: βIII-Tubulin; Red: Cofilin. Blue: DAPI. Scale bar = 30 μm. Data are expressed as mean ± SEM. $^{**}p < 0.01$; $^{***}p < 0.001$.

One neuron from each experimental condition is shown, and rods are indicated (arrows) in cells incubated with Aβ oligomers (Figure 3). Furthermore, the protective effect of S100B displayed a dose-dependent response (Supplementary Figure 3). Moreover, the comparable number of cells with rods induced by Aβ at 24 and 48 h (Supplementary Figure 3) suggests that S100B reverses rod formation rather than preventing it. These findings indicate that S100B protects against early cytoskeleton alterations triggered by Aβ oligomers, potentially mitigating disease progression. The observed protection may also result from its other functions on neuronal homeostasis.

3.4 S100B prevents synapse loss induced by Aβ42 oligomers in rat primary hippocampal neuron cultures

Aβ deposition in the brain leads to synaptic dysfunction by impairing neurotransmitter release and reuptake, reducing synaptic density and by triggering the formation of cofilin-actin rods, structures that inhibit intracellular trafficking and cause synaptic loss. To evaluate whether S100B directly impacts synaptic structures and can counteract the Aβ-induced dysfunction, primary cultures of rat hippocampal neurons were analyzed using immunocytochemistry for pre-and post-synaptic markers, VGLUT1 and PSD-95, respectively. As shown in Figure 4, treatment with Aβ oligomers (10 μM, 48 h) significantly reduced PSD-95 levels and the number of active synapses compared to the control. Remarkably, S100B treatment (5 μM, 24 h) rescued the Aβ-induced phenotype. S100B alone did not produce alterations, as compared to the control. These findings show that extracellular S100B mitigates Aβ-induced synaptic toxicity, consistent with its role as a molecular chaperone.

4 Discussion

AD is characterized by the extracellular deposition of aggregated Aβ peptide and the intracellular accumulation of Tau (Morris et al., 2022; Bu, 2009). Recent research has demonstrated that S100B, which has both intra and extracellular functions, can inhibit both the aggregation and toxicity of these proteins, even under sub-stoichiometric conditions (Cristóvão et al., 2018; Cristóvão et al., 2020; Rodrigues et al., 2021). The interaction between S100B and Aβ not only reverses the peptide's toxicity, which otherwise decreases cell viability and promotes apoptosis (Cristóvão et al., 2018), but also prevents Tau oligomers from seeding further aggregation into nearby cells (Moreira et al., 2021). These findings suggest that S100B acts in a chaperone-like capacity, mitigating the pathological effects of Aβ and Tau in AD.

However, the molecular and cellular mechanisms underlying S100B neuroprotective effects remain incompletely understood, particularly those involved in neuronal protection. In this study, we demonstrate that in AD mice S100B levels increase with age, not only in astrocytes but also in neurons. This suggests that neuronal S100B expression may play a role in counteracting the toxic effects of aggregating proteins, although we cannot rule out the possibility that part of the S100B detected in neurons is partially of astrocytic origin. This could reflect a component of neuron–glia crosstalk. Indeed, several studies have shown that astrocytes upregulate S100B expression with aging and in AD models, particularly in regions adjacent to Aβ plaques (Mrak and Griffin, 2001).

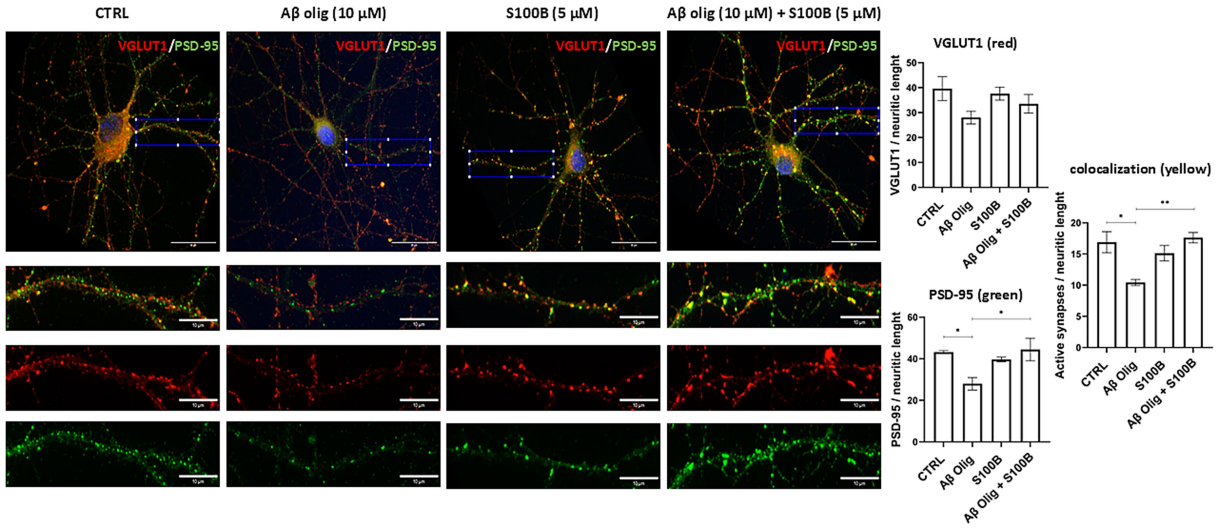

FIGURE 4
Impact of S100B and Aβ oligomers in synaptic structures of primary cultures of rat hippocampal neurons. Representative images and quantification plots of rat hippocampal neurons (DIV14) showing pre-(VGLUT1) and pos- (PSD-95) synaptic markers staining, and active synapses assessed by the colocalization of VGLUT1 and PSD-95; Treatment with Aβ oligomers (Aβ Olig, 10 μM) induces a significant decrease in PSD-95 and active synapses, as compared to control, and S100B (5 μM) rescues the Aβ-induced phenotype. S100B alone did not produce alterations, as compared to control (CTRL). Blue: DAPI; Red: VGLUT1; Green: PSD-95; Enlarged insertion (scale bar = 10 μm) corresponds to the area defined by the blue rectangle in the top panels (scale bar = 30 μm) and was used to the quantification. Data are expressed as mean ± SEM. *$p < 0.05$; **$p < 0.01$.

To further investigate the contribution of neuronal S100B against Aβ toxicity, we examined various Aβ conditions, including different species, concentrations, and incubation times, and found that only oligomers at 10 μM and incubated for 24 h significantly increased S100B expression in SH-SY5Y cells. This is particularly interesting, as oligomers are widely considered the most toxic Aβ species compared to their soluble or fibrillar counterparts (Lee et al., 2017). Notably, these neuronal cells also secreted S100B into the medium, indicating that S100B-producing neurons may help protect neighboring neurons.

The AβPPswe/PS1A246E AD mouse model employed in this study presents cofilin-actin rod formation, as observed in the brains of AD patients (Sisodia and Price, 1995). Cofilin is a protein that binds actin, modulating its transport and functioning. Toxic stimuli, such as Aβ, disrupts this interaction, leading to the formation of cofilin-actin rods. These structures cause cytoskeletal dysregulation and synaptic impairment, ultimately compromising cell viability (Davis et al., 2009; Bernstein and Bamburg, 2010). Using primary rat hippocampal neuron cultures treated with Aβ oligomers, we recapitulated cofilin pathology and demonstrated that S100B partially reversed rod formation, thereby helping to preserve cytoskeletal integrity.

Another consequence of Aβ peptide deposition is synaptic dysfunction, which disrupts neurotransmitter release and reuptake, leading to reduced synaptic density. Studies in Wistar rats have shown that an intracerebroventricular injection of Aβ oligomers results in a decrease in synaptic density, structure and activity (Freir et al., 2011). Aβ can also block axonal transport (Rui et al., 2006), impair synaptic vesicle dynamics (Shankar and Walsh, 2009; Marsh and Alifragis, 2018), and interfere with receptors in the synaptic space. Additionally, Aβ-induced dystrophic axons are linked to disruptions in the pre-synaptic machinery (Miledi and Slater, 1970; Hudson et al., 1984; Gillingwater and Ribchester, 2001; Pun et al., 2006), further inhibiting neurotransmitter release and impairing synaptic function. To assess the impact of extracellular S100B in synapses, we evaluated pre- and post-synaptic markers and their co-localization to measure active synapses. Our results showed that S100B protected against the deleterious effects of Aβ, while S100B alone did not affect the synaptic structures, suggesting that its protective effect is specifically related to its ability to mitigate Aβ toxicity. In this context, cytoskeleton changes triggered by Aβ lead to the formation of cofilin-actin rods, causing synaptic damage. However, S100B, through its interaction with Aβ, prevents this sequence of events and protects synaptic integrity.

In summary, our study presents compelling evidence supporting the neuroprotective role of S100B, demonstrated both in cells *in vitro* and in the AβPPswe/PS1A246E AD mouse model. We reveal that S100B safeguards neurons by preventing the formation of cytoskeletal-disrupting cofilin-actin rods and protecting synaptic structures. Nevertheless, whether only neuronal S100B is responsible for protection in AD is not known and further investigation is necessary.

Data availability statement

The original contributions presented in the study are included in the article/Supplementary material, further inquiries can be directed to the corresponding author.

Ethics statement

The animal study was approved by Institute for Research and Innovation in Health Sciences (i3S) Animal Ethics Committee. The study was conducted in accordance with the local legislation and institutional requirements.

Author contributions

JS: Writing – review & editing, Formal analysis, Writing – original draft, Investigation. MN: Investigation, Writing – review & editing, Formal analysis. AF: Writing – review & editing, Methodology. MO: Supervision, Writing – review & editing. TG: Writing – review & editing, Methodology. JO: Methodology, Writing – review & editing. ML: Writing – review & editing, Conceptualization, Supervision. CMG: Supervision, Conceptualization, Writing – review & editing, Writing – original draft, Funding acquisition. IC: Writing – review & editing, Validation, Project administration, Conceptualization, Writing – original draft, Supervision, Funding acquisition.

Funding

The author(s) declare that financial support was received for the research and/or publication of this article. This work was funded by FCT – Fundação para a Ciência e Tecnologia (Portugal) through research grants PTDC/MED-PAT/0959/2021 (DOI: 10.54499/PTDC/MED-PAT/0959/2021; to IC), centre grant UID/04046/2025 - Instituto de Biosistemas & Ciências Integrativas and Ph. D. fellowships 2023.03111. BD (to JS); BD/06393/2021 (to AF) and 2020.07444. BD (to TG), and master fellowship Fellow BI/FCT_Prep2020/i3S/26102711/2023 (to JO). The work was also funded by the European Union (TWIN2PIPSA, GA 101079147 to CMG). Views and opinions expressed are, however, those of the author(s) only and do not necessarily reflect those of the European Union or European Research Executive Agency (REA). Neither the European Union nor the granting authority can be held responsible for them. MIOS is supported by 2023.08100. CEECIND. MAL was supported by CEECINST/00091/2018.

Acknowledgments

The authors acknowledge the support of the i3S Scientific Platforms, Advanced Light Microcopy (ALM), member of the national infrastructure PPBI–Portuguese Platform of Bioimaging (PPBI-POCI-01-0145-FEDER-022122), Histology and Electron Microscopy platform, Cell Culture and Genotyping platform and the i3S Animal Facility. The content of the manuscript has previously appeared online in a preprint: bioRxiv 2025.04.04.647260; doi: https://doi.org/10.1101/2025.04.04.647260.

Conflict of interest

The authors declare that the research was conducted in the absence of any commercial or financial relationships that could be construed as a potential conflict of interest.

The author(s) declared that they were an editorial board member of Frontiers, at the time of submission. This had no impact on the peer review process and the final decision.

Generative AI statement

The author(s) declare that no Gen AI was used in the creation of this manuscript.

Publisher's note

Supplementary material

The Supplementary material for this article can be found online at: https://www.frontiersin.org/articles/10.3389/fnmol.2025.1636365/full#supplementary-material

References

Bamburg, J., Minamide, L., Wiggan, O., Tahtamouni, L., and Kuhn, T. (2021). Cofilin and actin dynamics: multiple modes of regulation and their impacts in neuronal development and degeneration. *Cells* 10:2726. doi: 10.3390/cells10102726

Benilova, I., Karran, E., and De Strooper, B. (2012). The toxic aβ oligomer and Alzheimer's disease: an emperor in need of clothes. *Nat. Neurosci.* 15, 349–357. doi: 10.1038/nn.3028

Bernstein, B. W., and Bamburg, J. R. (2010). ADF/Cofilin: a functional node in cell biology. *Trends Cell Biol.* 20, 187–195. doi: 10.1016/j.tcb.2010.01.001

Bernstein, B. W., Shaw, A. E., Minamide, L. S., Pak, C. W., and Bamburg, J. R. (2012). Incorporation of Cofilin into rods depends on disulfide intermolecular bonds: implications for actin regulation and neurodegenerative disease. *J. Neurosci.* 32, 6670–6681. doi: 10.1523/JNEUROSCI.6020-11.2012

Borchelt, D. R., Ratovitski, T., Van Lare, J., Lee, M. K., Gonzales, V., Jenkins, N. A., et al. (1997). Accelerated amyloid deposition in the brains of transgenic mice coexpressing mutant presenilin 1 and amyloid precursor proteins. *Neuron* 19, 939–945.

Botelho, H. M., Fritz, G., and Gomes, C. M. (2012). Analysis of S100 Oligomers and Amyloids. In: Sigurdsson, E., Calero, M., Gasset, M. (eds.) *Amyloid Proteins*. Methods in Molecular Biology, Humana Press. 849, 373–386. doi: 10.1007/978-1-61779-551-0_25

Bu, G. (2009). Apolipoprotein E and its receptors in Alzheimer's disease: pathways, pathogenesis and therapy. *Nat Rev Neurosci.* 10, 333–344. doi: 10.1038/nrn2620

Cichon, J., Sun, C., Chen, B., Jiang, M., Chen, X. A., Sun, Y., et al. (2012). Cofilin aggregation blocks intracellular trafficking and induces synaptic loss in hippocampal neurons. *J. Biol. Chem.* 287, 3919–3929. doi: 10.1074/jbc.M111.301911

Cline, E. N., Bicca, M. A., Viola, K. L., and Klein, W. L. (2018). The amyloid-β oligomer hypothesis: beginning of the third decade. *J Alzheimer's Dis* 64, S567–S610. doi: 10.3233/JAD-179941

Costa, R., Gonçalves, A., Saraiva, M. J., and Cardoso, I. (2008). Transthyretin binding to A-Beta peptide - impact on A-Beta fibrillogenesis and toxicity. *FEBS Lett.* 582, 936–942. doi: 10.1016/j.febslet.2008.02.034

Cristóvão, J. S., Figueira, A. J., Carapeto, A. P., Rodrigues, M. S., Cardoso, I., and Gomes, C. M. (2020). The S100B Alarmin is a dual-function chaperone suppressing amyloid-β oligomerization through combined zinc chelation and inhibition of protein aggregation. *ACS Chem. Neurosci.* 11, 2753–2760. doi: 10.1021/acschemneuro.0c00392

Cristóvão, J. S., Morris, V. K., Cardoso, I., Leal, S. S., Martínez, J., Botelho, H. M., et al. (2018). The neuronal S100B protein is a calcium-tuned suppressor of amyloid-β aggregation. *Sci. Adv.* 4:eaaq1702.13. doi: 10.1126/sciadv.aaq1702

Cristóvão, J. S., Santos, R., and Gomes, C. M. (2016). Metals and neuronal metal binding proteins implicated in Alzheimer's disease. *Oxidative Med. Cell. Longev.* 9812178:13. doi: 10.1155/2016/9812178

Cuello, A. C. (2017). Early and late CNS inflammation in Alzheimer's disease: two extremes of a continuum? *Trends Pharmacol. Sci.* 38, 956–966. doi: 10.1016/j.tips.2017.07.005

Davis, R. C., Maloney, M. T., Minamide, L. S., Flynn, K. C., Stonebraker, M. A., and Bamburg, J. R. (2009). Mapping cofilin-actin rods in stressed hippocampal slices and the role of cdc42 in amyloid-β-induced rods. *J Alzheimer's Dis* 18, 35–50. doi: 10.3233/JAD-2009-1122

De Felice, F. G., Velasco, P. T., Lambert, M. P., Viola, K., Fernandez, S. J., Ferreira, S. T., et al. (2007). Aβ oligomers induce neuronal oxidative stress through an N-methyl-D-aspartate receptor-dependent mechanism that is blocked by the Alzheimer drug Memantine. *J. Biol. Chem.* 282, 11590–11601. doi: 10.1074/jbc.M607483200

Decker, H., Lo, K. Y., Unger, S. M., Ferreira, S. T., and Silverman, M. A. (2010). Amyloid- peptide oligomers disrupt axonal transport through an NMDA receptor-dependent mechanism that is mediated by glycogen synthase kinase 3 in primary cultured hippocampal neurons. *J. Neurosci.* 30, 9166–9171. doi: 10.1523/JNEUROSCI.1074-10.2010

Donato, R., Sorci, G., Riuzzi, F., Arcuri, C., Bianchi, R., Brozzi, F., et al. (2009). S100B's double life: intracellular regulator and extracellular signal. *Biochim. Biophys. Acta, Mol. Cell Res.* 1793, 1008–1022. doi: 10.1016/j.bbamcr.2008.11.009

Fanò, G., Biocca, S., Fulle, S., Mariggiò, M. A., Belia, S., and Calissano, P. (1995). The S-100: a protein family in search of a function. *Prog. Neurobiol.* 46, 71–82.

Forloni, G., and Balducci, C. (2018). Alzheimer's disease, oligomers, and inflammation. *J Alzheimer's Dis* 62, 1261–1276. doi: 10.3233/JAD-170819

Freir, D. B., Fedriani, R., Scully, D., Smith, I. M., Selkoe, D. J., Walsh, D. M., et al. (2011). Aβ oligomers inhibit synapse remodelling necessary for memory consolidation. *Neurobiol. Aging* 32, 2211–2218. doi: 10.1016/j.neurobiolaging.2010.01.001

Gillingwater, T. H., and Ribchester, R. R. (2001). Compartmental neurodegeneration and synaptic plasticity in the Wld s mutant mouse. *J. Physiol.* 534, 627–639. doi: 10.1111/j.1469-7793.2001.00627.x

Gonzalez, L. L., Garrie, K., and Turner, M. D. (2020). Role of S100 proteins in health and disease. *Biochim. Biophys. Acta, Mol. Cell Res.* 1867:118677. doi: 10.1016/j.bbamcr.2020.118677

Hagmeyer, S., Cristóvão, J. S., Mulvihill, J. J. E., Boeckers, T. M., Gomes, C. M., and Grabrucker, A. M. (2018). Zinc binding to S100B affords regulation of trace metal homeostasis and excitotoxicity in the brain. *Front. Mol. Neurosci.* 10:456. doi: 10.3389/fnmol.2017.00456/full

Hagmeyer, S., Romão, M. A., Cristóvão, J. S., Vilella, A., Zoli, M., Gomes, C. M., et al. (2019). Distribution and relative abundance of S100 proteins in the brain of the APP23 Alzheimer's disease model mice. *Front. Neurosci.* 13:640.10. doi: 10.3389/fnins.2019.00640

Hardy, J. A., and Higgins, G. A. (1992). Alzheimer's disease: the amyloid cascade hypothesis. *Science* 256, 184–185.

Heneka, M. T., Carson, M. J., Landreth, G. E., Brosseron, F., and Feinstein, D. L. (2015). Neuroinflammation in Alzheimer's disease. *Lancet Neurol.* 14, 388–405. doi: 10.1016/S1474-4422(15)70016-5

Hernández-Ortega, K., Canul-Euan, A. A., Solis-Paredes, J. M., Borboa-Olivares, H., Reyes-Muñoz, E., Estrada-Gutierrez, G., et al. (2024). S100B actions on glial and neuronal cells in the developing brain: an overview. *Front. Neurosci.* 4:18. doi: 10.3389/fnins.2024.1425525/full

Holtzman, D. M., Morris, J. C., and Goate, A. M. (2011). Alzheimer's disease: the challenge of the second century. *Sci. Transl. Med.* 3:77sr1.35. doi: 10.1126/scitranslmed.3002369

Hudson, S., Hudson, C., Deshpande, S. S., and Albuquerque, E. X. (1984). Consequences of axonal transport blockade by batrachotoxin on mammalian neuromuscular junction. III. An ultrastructural study. *Brain Res.* 296, 319–332.

Knowles, T. P. J., Vendruscolo, M., and Dobson, C. M. (2014). The amyloid state and its association with protein misfolding diseases. *Nat. Rev. Mol. Cell Biol.* 15, 384–396. doi: 10.1038/nrm3810

Lacor, P. N., Buniel, M. C., Furlow, P. W., Sanz Clemente, A., Velasco, P. T., Wood, M., et al. (2007). Aβ oligomer-induced aberrations in synapse composition, shape, and density provide a molecular basis for loss of connectivity in Alzheimer's disease. *J. Neurosci.* 27, 796–807. doi: 10.1523/JNEUROSCI.3501-06.2007

Lazzari, C., Kipanyula, M. J., Agostini, M., Pozzan, T., and Fasolato, C. (2015). Aβ42 oligomers selectively disrupt neuronal calcium release. *Neurobiol. Aging* 36, 877–885. doi: 10.1016/j.neurobiolaging.2014.10.020

Lee, S. J. C., Nam, E., Lee, H. J., Savelieff, M. G., and Lim, M. H. (2017). Towards an understanding of amyloid-β oligomers: characterization, toxicity mechanisms, and inhibitors. *Chem. Soc. Rev.* 46, 310–323. doi: 10.1039/C6CS00731G

Li, C., Zhao, R., Gao, K., Wei, Z., Yaoyao Yin, M., Ting Lau, L., et al. (2011). Astrocytes: implications for Neuroinflammatory pathogenesis of Alzheimers disease. *Curr. Alzheimer Res.* 8, 67–80. doi: 10.2174/156720511794604543

Livak, K. J., and Schmittgen, T. D. (2001). Analysis of relative gene expression data using real-time quantitative PCR and the 2−ΔΔCT method. *Methods* 25, 402–408. doi: 10.1006/meth.2001.1262

Ma, Q.-L., Yang, F., Rosario, E. R., Ubeda, O. J., Beech, W., Gant, D. J., et al. (2009). Amyloid oligomers induce phosphorylation of tau and inactivation of insulin receptor substrate via c-Jun N-terminal kinase signaling: suppression by Omega-3 fatty acids and curcumin. *J. Neurosci.* 29, 9078–9089. doi: 10.1523/JNEUROSCI.1071-09.2009

Maloney, M. T., Minamide, L. S., Kinley, A. W., Boyle, J. A., and Bamburg, J. R. (2005). B-Secretase-cleaved amyloid precursor protein accumulates at actin inclusions induced in neurons by stress or amyloid β: a feedforward mechanism for Alzheimer's disease. *J. Neurosci.* 25, 11313–11321. doi: 10.1523/JNEUROSCI.3711-05.2005

Marsh, J., and Alifragis, P. (2018). Synaptic dysfunction in Alzheimer's disease: the effects of amyloid beta on synaptic vesicle dynamics as a novel target for therapeutic intervention. *Neural Regen. Res.* 13:616. doi: 10.4103/1673-5374.230276

Marshak, D. R., Pesce, S. A., Stanley, L. C., and Griffin, W. S. T. (1992). Increased S100β neurotrophic activity in Alzheimer's disease temporal lobe. *Neurobiol. Aging* 13, 1–7.

Michaels, T. C. T., Šarić, A., Habchi, J., Chia, S., Meisl, G., Vendruscolo, M., et al. (2018). Chemical kinetics for bridging molecular mechanisms and macroscopic measurements of amyloid fibril formation. *Annu. Rev. Phys. Chem.* 69, 273–298. doi: 10.1146/annurev-physchem-050317-021322

Miledi, R., and Slater, C. R. (1970). On the degeneration of rat neuromuscular junctions after nerve section. *J. Physiol.* 207, 507–528.

Moreira, G. G., Cantrelle, F.-X., Quezada, A., Carvalho, F. S., Cristóvão, J. S., Sengupta, U., et al. (2021). Dynamic interactions and Ca2+−binding modulate the holdase-type chaperone activity of S100B preventing tau aggregation and seeding. *Nat. Commun.* 12:6292. doi: 10.1038/s41467-021-26584-2

Morris, J. C., Weiner, M., Xiong, C., Beckett, L., Coble, D., Saito, N., et al. (2022). Autosomal dominant and sporadic late onset Alzheimer's disease share a common in vivo pathophysiology. *Brain* 145, 3594–3607. doi: 10.1093/brain/awac181

Mrak, R. (2001). The role of activated astrocytes and of the neurotrophic cytokine S100B in the pathogenesis of Alzheimer's disease. *Neurobiol. Aging* 22, 915–922. doi: 10.1016/S0197-4580(01)00293-7

Mrak, R., and Griffin, W. S. (2001). Interleukin-1, neuroinflammation, and Alzheimer's disease. *Neurobiol. Aging* 22, 903–908. doi: 10.1016/s0197-4580(01)00287-1

Namme, J. N., Bepari, A. K., and Takebayashi, H. (2021). Cofilin signaling in the CNS physiology and neurodegeneration. *Int. J. Mol. Sci.* 22:10727. doi: 10.3390/ijms221910727

Oliveira da Silva, M. I., Santejo, M., Babcock, I. W., Magalhães, A., Minamide, L. S., Won, S.-J., et al. (2024). A-Synuclein triggers cofilin pathology and dendritic spine impairment via a PrPC-CCR5 dependent pathway. *Cell Death Dis.* 15:264. doi: 10.1038/s41419-024-06630-9

Oliveira, S. M., Ribeiro, C. A., Cardoso, I., and Saraiva, M. J. (2011). Gender-dependent transthyretin modulation of brain amyloid-β levels: evidence from a mouse model of alzheimer's disease. *J Alzheimer's Dis* 27, 429–439. doi: 10.3233/JAD-2011-110488

Ostendorp, T., Heizmann, C. W., Kroneck, P. M. H., and Fritz, G. (2005). Purification, crystallization and preliminary X-ray diffraction studies on human ca 2+ −binding protein S100B. *Acta Crystallogr. Sect. F Struct. Biol. Cryst. Commun.* 61, 673–675. doi: 10.1107/S1744309105018014

Pun, S., Santos, A. F., Saxena, S., Xu, L., and Caroni, P. (2006). Selective vulnerability and pruning of phasic motoneuron axons in motoneuron disease alleviated by CNTF. *Nat. Neurosci.* 9, 408–419. doi: 10.1038/nn1653

Rodrigues, F. E. P., Figueira, A. J., Gomes, C. M., and Machuqueiro, M. (2021). Computational analysis of the interactions between the S100B extracellular chaperone and its amyloid β peptide client. *Int. J. Mol. Sci.* 22:3629. doi: 10.3390/ijms22073629

Rui, Y., Tiwari, P., Xie, Z., and Zheng, J. Q. (2006). Acute impairment of mitochondrial trafficking by β-amyloid peptides in hippocampal neurons. *J. Neurosci.* 26, 10480–10487. doi: 10.1523/JNEUROSCI.3231-06.2006

Schindelin, J., Arganda-Carreras, I., Frise, E., Kaynig, V., Longair, M., Pietzsch, T., et al. (2012). Fiji: an open-source platform for biological-image analysis. *Nat. Methods* 9, 676–682. doi: 10.1038/nmeth.2019

Schützmann, M. P., Hasecke, F., Bachmann, S., Zielinski, M., Hänsch, S., Schröder, G. F., et al. (2021). Endo-lysosomal aβ concentration and pH trigger formation of aβ oligomers that potently induce tau missorting. *Nat. Commun.* 12:4634. doi: 10.1038/s41467-021-24900-4

Selkoe, D. J., and Hardy, J. (2016). The amyloid hypothesis of Alzheimer's disease at 25 years. *EMBO Mol. Med.* 8, 595–608. doi: 10.15252/emmm.201606210

Shankar, G. M., and Walsh, D. M. (2009). Alzheimer's disease: synaptic dysfunction and aβ. *Mol. Neurodegener.* 4:48. doi: 10.1186/1750-1326-4-48

Sisodia, S. S., and Price, D. L. (1995). Role of the β-amyloid protein in Alzheimer's disease. *FASEB J.* 9, 366–370.

Wang, X., Wang, W., Li, L., Perry, G., Lee, H., and Zhu, X. (2014). Oxidative stress and mitochondrial dysfunction in Alzheimer's disease. *Biochim. Biophys. Acta Mol. basis Dis.* 1842, 1240–1247. doi: 10.1016/j.bbadis.2013.10.015

Williams, T. L., Johnson, B. R. G., Urbanc, B., Jenkins, A. T. A., Connell, S. D. A., and Serpell, L. C. (2011). Aβ42 oligomers, but not fibrils, simultaneously bind to and cause damage to ganglioside-containing lipid membranes. *Biochem. J.* 439, 67–77. doi: 10.1042/BJ20110750

Wurz, A. I., Schulz, A. M., O'Bryant, C. T., Sharp, J. F., and Hughes, R. M. (2022). Cytoskeletal dysregulation and neurodegenerative disease: formation, monitoring, and inhibition of cofilin-actin rods. *Front. Cell. Neurosci.* 16:74. doi: 10.3389/fncel.2022.982074/full